CrossMark

ARTICLE

Development and properties evaluation of Mg–6% Zn/Al multilayered composites processed by accumulative roll bonding

Gajanan Anne, Motagondanahalli Rangarasaiah Ramesh,[a] and Hanumanthappa Shivananda Nayaka
Department of Mechanical Engineering, National Institute of Technology Karnataka, Mangalore 575025, India

Shashi Bhushan Arya
Department of Metallurgical and Materials Engineering, National Institute of Technology Karnataka, Mangalore 575025, India

Sandeep Sahu
Department of Materials Science Engineering, Indian Institute of Technology Kanpur, Kanpur 208016, India

(Received 30 December 2016; accepted 18 April 2017)

Accumulative roll bonding (ARB) process was used to develop Mg–6% Zn/Al and Mg–6% Zn/anodized–Al multilayered composites. Microstructural characterization was done using scanning electron microscopy, energy-dispersive X-ray spectroscopy, electron backscattered diffraction, and transmission electron microscopy. An average grain size measured in the roll-bonded layers of Al, anodized Al, and Mg–2% Zn was found to be 1.8 μm, 1.6 μm, and 0.6 μm, respectively. Phases $Al_{17}Mg_{12}$, $AlMg_4Zn_{11}$, and Al_2O_3 after 5-pass of ARB were confirmed by X-ray diffraction analysis. The Mg–6% Zn/Al and Mg–6% Zn/anodized Al composites exhibited tensile strengths ~252 MPa and ~256 MPa, respectively, after a 5-pass ARB process. Hardness of the individual layers of composite increased linearly with an increase in the number of ARB passes. Fractographs of the multilayered composite illustrated the ductile failure in Al and anodized Al layers and transgranular brittle fracture in Mg–6% Zn layers.

I. INTRODUCTION

Metallic multilayered laminate composites have become more demanding in automotive, aerospace, medical, and electrical industries due to its unique physical and mechanical properties.[1] These composites are generally fabricated by coating techniques or by bonding techniques such as diffusion and adhesive. The deformation bonding can be utilized as an alternative approach for producing metallic multilayered composite with ultrafine grains (UFGs).[2]

Severe plastic deformation (SPD) is considered as an effective grain refinement technique to produce high strength in metallic materials.[3,4] Various SPD techniques are high pressure torsion,[5] equal-channel angular pressing (ECAP),[6,7] accumulative roll bonding process (ARB),[8–11] multiaxial forging (MAF),[12] and repetitive corrugation and straightening (RCS).[13] ARB technique is found to be the most suitable process for the production of bulk materials with UFG and develop to multilayered composites. In ARB processing, the function of the rolling step is to achieve simultaneous deformation and bonding of the adjacent metallic layers being rolled. Major advantages of ARB technique are the development of multilayered composites at low cost, high productivity, and defects-free microstructure. In this regard, multilayered sheets, composed of alternative layers of Al and Mg alloys, have received a great deal of attention because of their outstanding combination of corrosion resistance from the Al alloy and high specific strength and extraordinary light weight from the Mg alloy.[14,15] Recently the ARB process has been successfully adapted to fabricate various UFG multilayered composites including Al/Cu,[16] Al/Mg,[17,18] Ti/Ni,[19,20] Al/Ti,[21] and Cu/Ni.[12] However, very meager information is available in the literature about the combination of anodization treatment and ARB of Mg–Zn/Al multilayered composites. Generally, most metal matrix composites are developed using stir casting, spray forming, and powder metallurgy. Some major drawbacks of these techniques are agglomeration, nonuniform distribution, and poor wettability of reinforcement particle which lead to poor mechanical properties.[13] Normally, metal matrix composites are developed by squeeze casting, spray forming, and powder metallurgy methods. The limited application of these techniques in engineering industries is due to the occurrence of defects such as agglomeration and nonuniform distribution of reinforcement particles and also higher manufacturing cost due to costly equipment and complex processing routes.[22] To overcome these problems, Jamaati et al. (2010)[23] reported the combination of anodizing and ARB processes as a novel

Contributing Editor: Mathias Göken
[a]Address all correspondence to this author.
e-mail: ramesdmt@gmail.com
DOI: 10.1557/jmr.2017.176

https://doi.org/10.1557/jmr.2017.176 Published online by Cambridge University Press

 © Materials Research Society 2017

approach to produce high strength multilayered composites. Anodization process is to develop an alumina layer on the material followed by uniform dispersing alumina particle into the bulk of the material through rolling process which is the novel method of obtaining dispersion strengthening in the composite.

In the present work, efforts have been made to develop Mg–6% Zn/Al and Mg–6% Zn/anodized Al multilayered composites through the ARB process, thereby combining advantageous properties of both Mg–6% Zn alloy and Al and Al_2O_3. The roll of grain refinement and anodization treatment in improving mechanical properties has been discussed through microstructure evaluation.

II. MATERIALS AND METHOD

Cast ingot of Mg–6% Zn and Al was homogenized at ~400 °C for 24 h in a tubular furnace. Rolling was carried out in a laboratory rolling mill of diameter 110 mm with intermediate heating at 300 °C for 10 min with 0.25% reduction per pass to get a final thickness of about 1 mm. Mg–6% Zn alloy and Al were degreased with acetone, wire-brushed, and then stacked alternatively and held for 10 min at 300 °C in a furnace before being roll-bonded with 50% reduction to get a Mg–6% Zn/Al multilayered composite.

In the second system of material, anodization was carried out on a pure Al sheet before it is roll-bonded with Mg–6% Zn. Anodization of the Al sheet was carried out in 15% H_2SO_4 solution with an operating potential of 16 V at 3.5 A for 60 min at 18 °C adopted for forced circulation for the period of one hour, to obtain a uniform aluminum oxide film.[24] The thickness of the alumina layer was measured by using scanning electron microscopy (SEM). A Mg–2% Zn sheet was degreased with acetone and wire-brushed, after surface preparation the Mg–6% Zn was stacked alternatively with anodized Al. The stacked composite was preheated for 10 min at 300 °C in a furnace, and then roll-bonded using A 2Hi rolling mill (Buhler Ltd., Braunschweig, Germany) at 20 rpm with 50% reduction to get a Mg–6% Zn/anodized Al multilayered composite.

The microstructure characterization of multilayered composites was done by using scanning electron microscopy (SEM; JEOL JSM-6380LA, JEOL USA Ltd., Peabody, Massachusetts), electron backscattered diffraction (EBSD; JEOL JSM-7100F, JEOL USA Ltd.), and transmission electron microscopy (TEM; JEOL JEM-2100, JEOL USA Ltd.). Composite samples were sectioned along the normal direction (ND)–rolling direction (RD) plane and polished sequentially up to 2000 grit SiC paper using diamond paste. Etching was done using an acetic-picral solution. Phase analysis was done on RD–transverse direction (TD) plane using the X-ray diffraction (XRD) analysis. For the EBSD analysis, the RD–ND plane of the samples was electro-polished in Struers' AC2 electrolyte at 16 V for 60 s at −25 °C. The EBSD results were analyzed using HKL Channel 5 software.

The Vickers microhardness test was performed in Omnitech microhardness tester (Omni-tech, Maharashtra, India) on the TD plane using a load of 10 g with the dwell time of 11 s. The tensile test was carried out according to ASTM E8 M standard using Tinius Olsen Tensometer (Noida, India) at a constant cross head speed with an initial strain rate of 5×10^{-3} s^{-1}. Following the standard, gage length, radius of fillet, length, and width of the specimens were equal to 20 mm, 7 mm, 64 mm, and 10 mm respectively.

III. RESULTS AND DISCUSSION

A. Microstructural investigations

SEM micrographs of the 5-pass ARB processed Mg–6% Zn/anodized Al multilayered composite show 32 alternative layers of Mg–6% Zn and anodized Al depicted in Fig. 1. There were no cracks or de-lamination along the interfaces of the multilayer composite which indicates good bonding between Mg–6% Zn alloy and anodized Al but a slight waviness layer structure was observed. The thickness of the multilayered composite decreases with an increase in the number of ARB passes and finally, 5-pass ARB processed composite layer thickness was found to be in the range of 40–50 μm. The UFGs are depicted in the ARB processed Al layer [Fig. 1(a)], anodized Al layer [Fig. 1(b)], Mg–6% Zn layer [Fig. 1(c)] in the Mg–6% Zn/Al, and Mg–6% Zn/anodized Al multilayered composites. Energy dispersive spectroscopy data show alternate layers of Al (region I) and Mg–6% Zn (region II) at the interface of Mg–6% Zn and Al (region III). Grain refinement during ARB is due (i) the subdivision of the initial grains and the formation of the subgrain structure with low angle grain boundaries (LAGBs) by multidirectional slip, (ii) misorientation increase and gradual transformation of low angle boundaries (LABs) to high angle grain boundaries (HAGBs) by dislocation accumulation, and (iii) migration of new HAGBs and formation of a well-defined UFG structure.[25] A fraction of recrystallized grains increased with an increase in strain due to the higher rate of nucleation of new grains during recrystallization, which resulted in a relatively uniform microstructure with UFGs. The dynamic recovery and recrystallization are the reason for the UFG structure in the SPD processed metals.[26,27]

B. EBSD analysis

The EBSD based analysis of the Al layer (on the ND–RD plane) in the 5-pass ARB Mg–6% Zn/Al multilayered composites is shown in Fig. 2. Here, Fig. 2(a) shows the inverse pole figure (IPF) map where a standard stereographic triangle corresponds to various crystallographic directions indicated by various colors. The grains

https://doi.org/10.1557/jmr.2017.176 Published online by Cambridge University Press

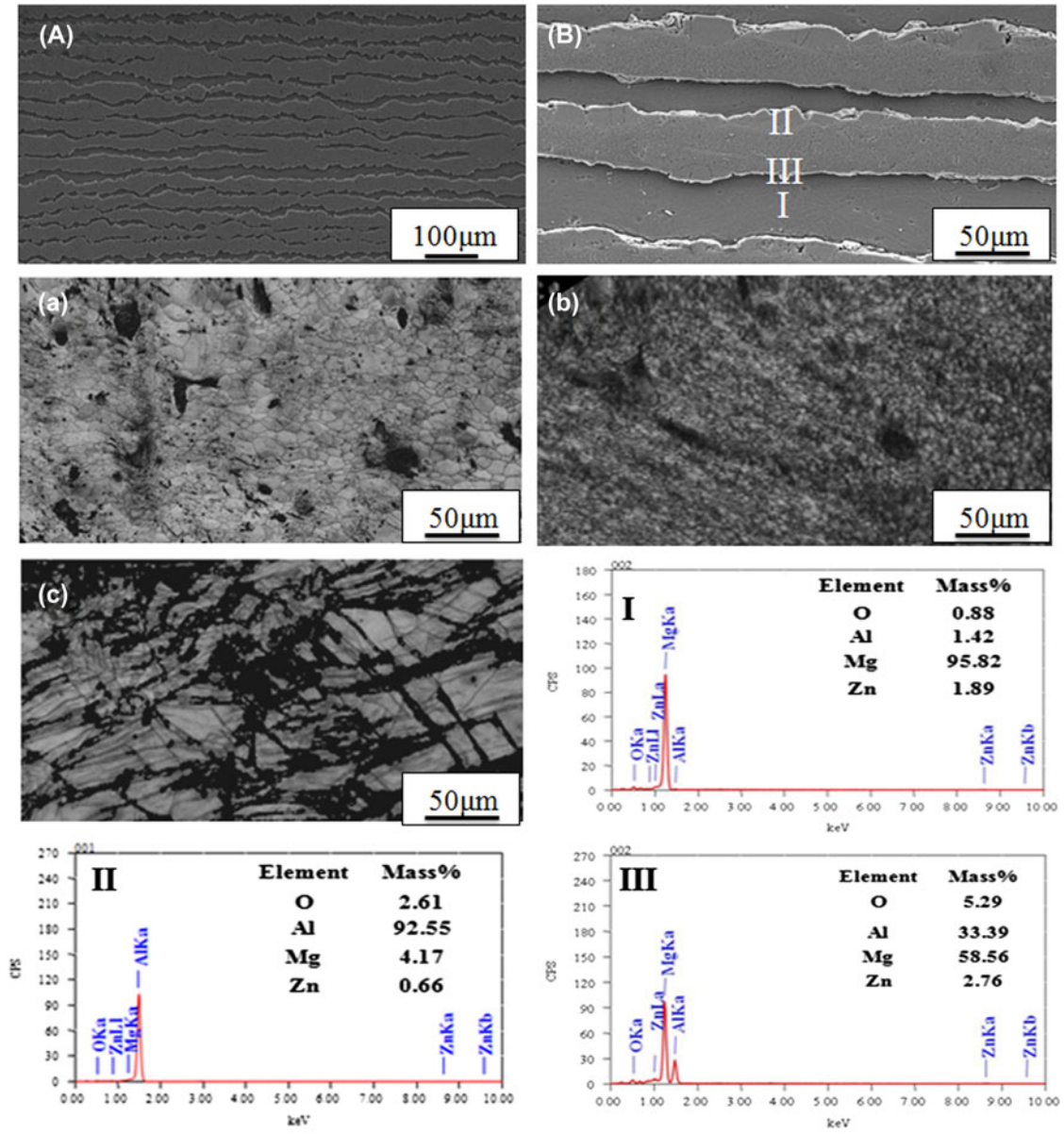


FIG. 1. SEM micrographs of (A) 5-pass ARB processed Mg–6% Zn/anodized Al multilayered composite, (B) magnified image. (a) Micrographs revealing the grains in Al layer, (b) anodized Al layer, (c) Mg–6% Zn layer; (I) EDS of the Mg–6% Zn layer, (II) anodized Al layer, (III) interphase between Mg–6% Zn/anodized Al layer.

are directed in the direction of rolling, which is ⟨001⟩ orientation. The misorientation angle distribution profile [Fig. 2(b)] revealed some fraction of HAGBs due to a large strain during deformation process [the density of dislocations increases which results in an increase in the fraction of high angle boundaries (HABs)].[28] If the number of ARB passes increases, the density of dislocations increases which results in an increase in the fraction of HABs. At the higher ARB passes, the area of grain boundaries increased due to internal energy in the deformed material.[29]

The grain boundary map overlaid with twins is shown in Fig. 2(c). Here, LABs are represented in green lines with misorientations between 2 and 15° and HABs are represented in black lines with misorientations above 15° and twins are marked in red colors. The Al layer in the multilayered composite which consists of fully equiaxed grains oriented in the rolling direction with a fraction of HABs are formed due to dynamic recrystallization during the ARB process. At higher strain, the LAGBs were converted into HAGBs. The percentage of twins has been calculated from the HKL channel 5 software (JEOL USA Ltd.) and found to be 2.39% and occurs along with some shear bands. The average grain size was found to be 1.8 μm as plotted in Fig. 2(d).

https://doi.org/10.1557/jmr.2017.176 Published online by Cambridge University Press

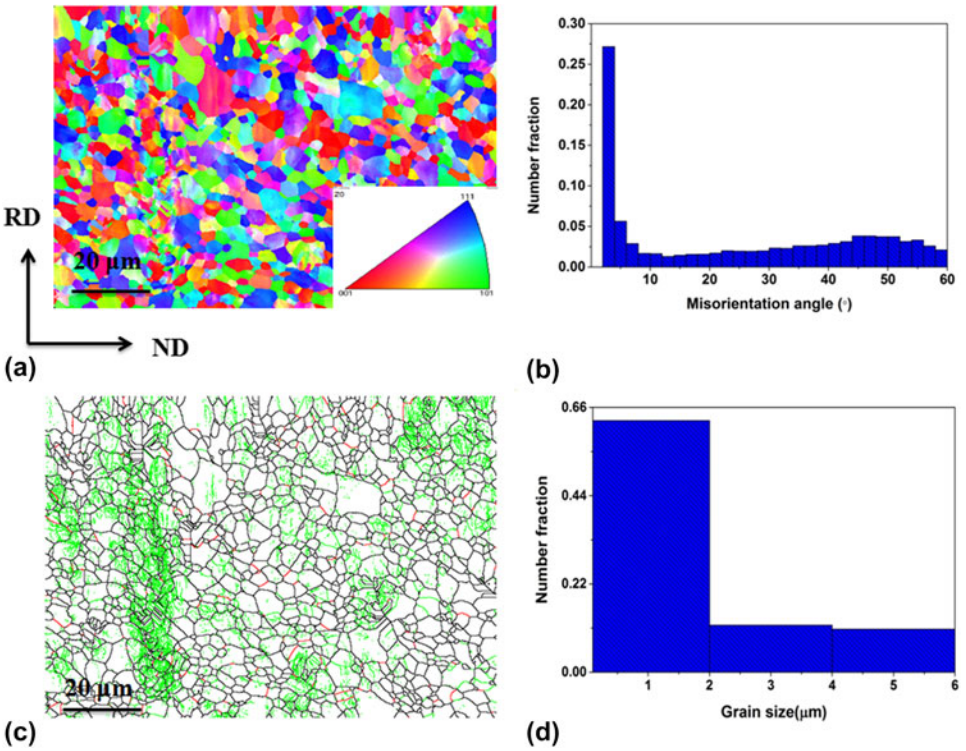


FIG. 2. EBSD based analysis of Al layer in the Mg–6% Zn/Al multilayered composite: (a) IPF map, (b) misorientation angle distribution profile, (c) IPF map and grain boundary map with twins, (d) grain size distribution.

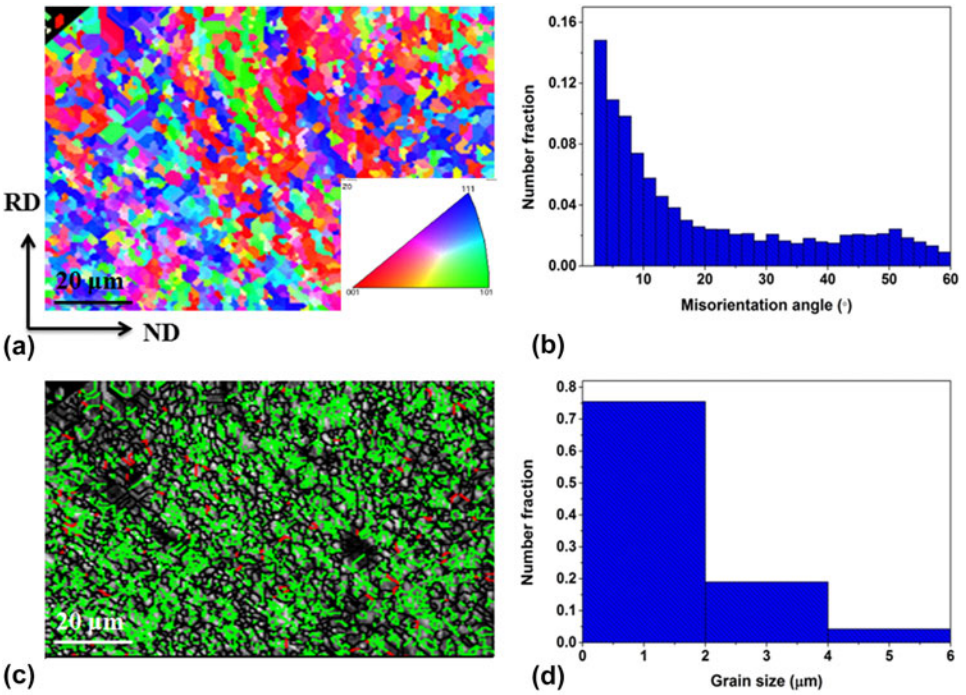


FIG. 3. EBSD based analysis of anodized Al layer in the Mg–6% Zn/anodized Al multilayered composite: (a) IPF map, (b) misorientation angle distribution profile, (c) IPF map overlaid with grain boundaries and twins, (d) grain size distribution.

Figure 3 depicts the EBSD based analysis of the anodized Al layer (taken on the ND–RD plane) in the Mg–6% Zn/anodized Al multilayered composite. The IPF map [Fig. 3(a)] revealed that the anodized Al layer grains are directed uniformly in ⟨001⟩ orientation in the direction of rolling. The misorientation angle distribution

https://doi.org/10.1557/jmr.2017.176 Published online by Cambridge University Press

profile [Fig. 3(b)] consists of subgrains with a fraction of HABs due of the dynamic recrystallization during ARB process. A grain boundary map overlaid with twins is shown in Fig. 3(c) which consists of equiaxed grains with some fraction of HABs. The percentage of twins was found to be 1.4%. The grain size variation profile [Fig. 3(d)] exhibited average grain size ~1.6 μm.

Figure 4 depicts the EBSD based analysis of the Mg–6% Zn layer (ND–RD plan) in the multilayered composites. The IPF map [Fig. 4(a)] revealed that Mg–6% Zn layer grains are directed uniformly in ⟨0001⟩ orientation in the direction of rolling. The misorientation angle distribution profile [shown in Fig. 4(b)] exhibited both LAGBs and HAGBs in Mg–6% Zn layer in the multilayered composite.

Figure 4(c) shows uniform distribution of UFGs and did not show any twin boundary. The grain size variation profile [Fig. 4(d)] exhibited average grain size ~0.6 μm. The fraction of recrystallized grains increased with an increase in strain due to the higher rate of nucleation of new grains during recrystallization, which resulted in a relatively uniform microstructure with fine grains. Mg–6% Zn layer did not show any twin boundary because when the grain size decreases, the twin nucleation decreases in the Mg alloys. In the fine grained Mg alloys, slips are activated resulting in the suppression of twin generation and reduction in mechanical anisotropy by grain refinement.[30] Deformation twins disappear in the Mg alloys, when the average grain size reaches <2 μm.

C. TEM analysis

TEM micrographs of the Mg–6% Zn/Al and Mg–6% Zn/anodized Al multilayered composites revealed fine grains with a high degree of misorientation [Figs. 5(a) and 5(b)]. The density of dislocations can be observed inside the grains. During the ARB process, due to high strain, subdivision of grains occurs due to the formation of planar dislocation boundaries and incidental dislocation boundaries. Higher misorientations form across these dislocation boundaries and spacing of boundaries reduces, which helps to create fine grains. The selected area electron diffraction (SAED) patterns revealed the formation of rings, which confirms the fine grain structure in the multilayered composites. Grain refinement is because of dynamic recrystallization as evidenced by the presence of equiaxed grains.

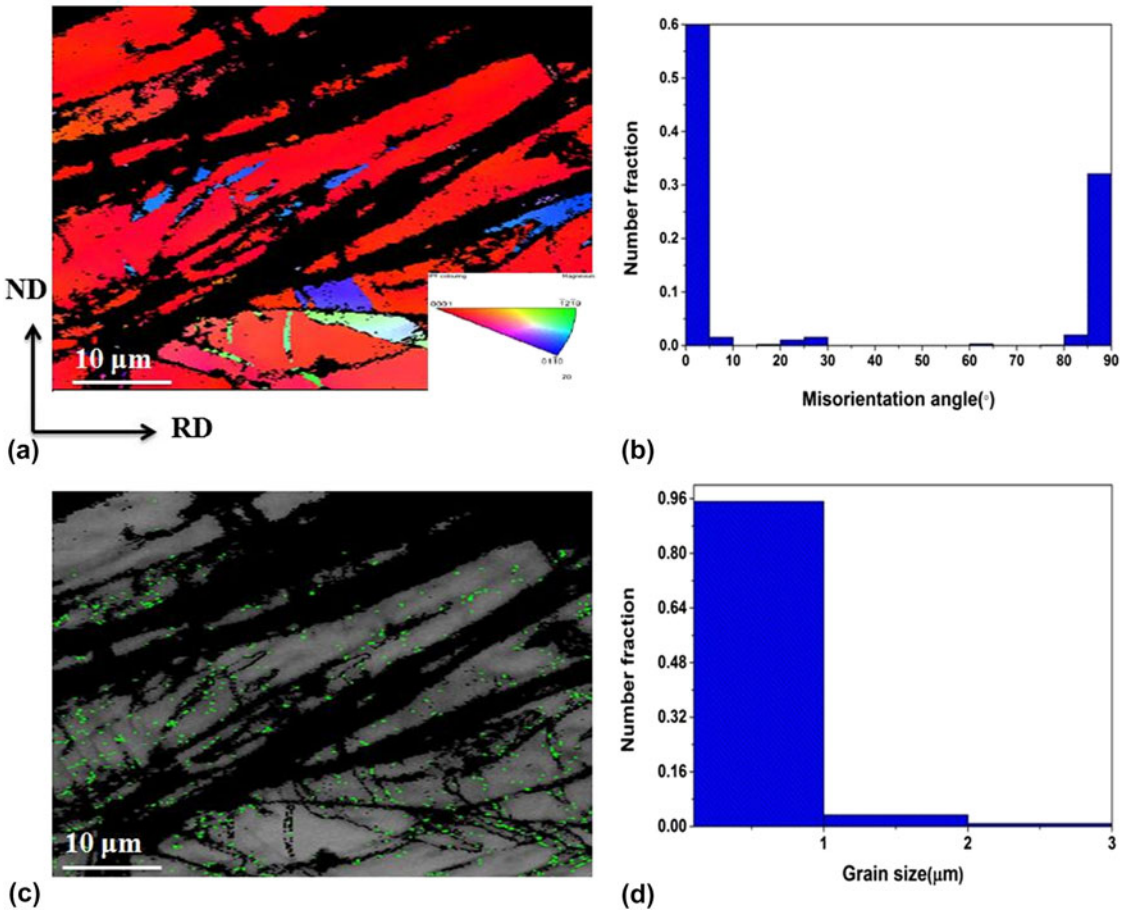


FIG. 4. EBSD based analysis of Mg–6% Zn layer in the multilayered composite: (a) IPF map, (b) grain boundary map overlaid with twins, (c) misorientation angle distribution profile, (d) grain size distribution.

https://doi.org/10.1557/jmr.2017.176 Published online by Cambridge University Press

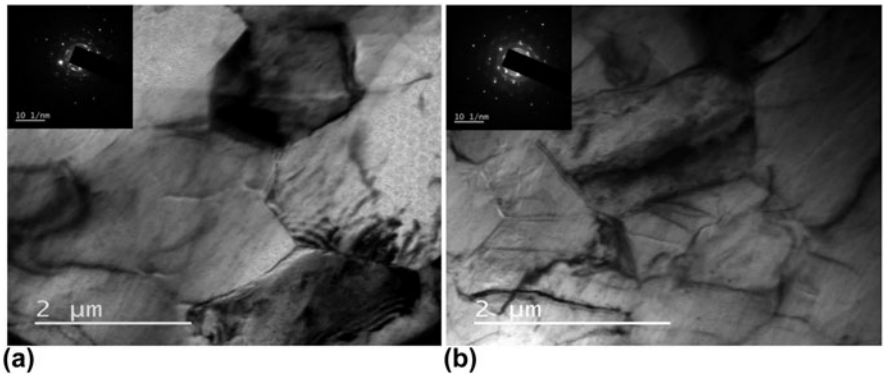


FIG. 5. TEM micrographs and SAED patterns of the 5-pass ARB processed (a) Mg–6% Zn/Al and (b) Mg–6% Zn/anodized Al multilayered composites.

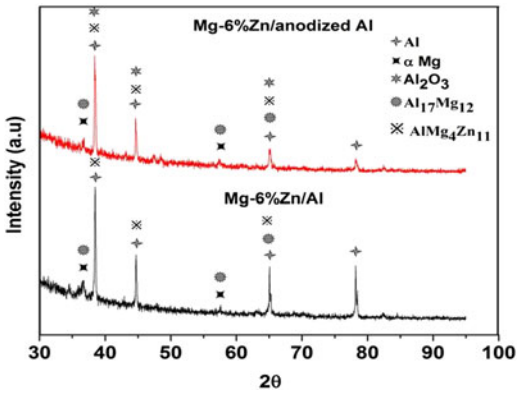


FIG. 6. XRD analysis along the cross section of ARB processed multilayered composite.

D. XRD

XRD patterns (Fig. 6) of the 5-pass ARB processed multilayered composites revealed peaks indexed to Al, αMg, $Al_{17}Mg_{12}$, and $AlMg_4Zn_{11}$. Multilayered composite exhibited intermetallic compounds due to inter diffusion between Al, Mg, and Zn because of high strain during ARB at 300 °C. The Mg–6% Zn/anodized Al multilayered composite exhibited Al_2O_3 peak due to anodization on the Al sheet before the ARB process.

E. Density

Density test was carried out according to Archimedes principle. The weight of the samples was measured in the presence of air and in water. Density test results are illustrated in Table I.

Developed Mg–6% Zn/Al and Mg–6% Zn/anodized Al multilayered composites were found to be 1.27 times light weight as compared to pure Al.

F. Microhardness

The microhardness variation of layered composite (Fig. 7) depicted that as the number of ARB passes increases, the microhardness of Mg–6% Zn, Al, and anodized Al layers increases. During initial passes of ARB process, the improvement of hardness was attributed to strain hardening (based on the density of dislocations and interactions between them) during the ARB process.

TABLE I. Density test results.

Materials	Density (kg/m^3)
Mg–6% Zn alloy	1781
Al sheet	2691
Anodized Al sheet	2696
Mg–6% Zn/Al composite	2109
Mg–6% Zn/anodized Al composite	2112

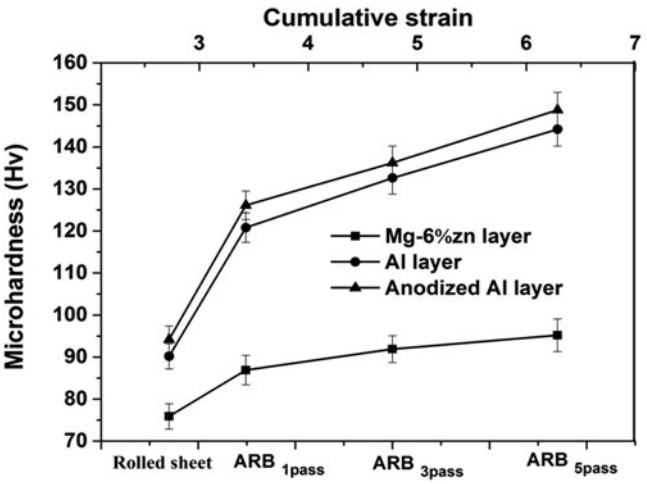


FIG. 7. Microhardness variation of composite layers of the Mg–6% Zn, Al, and anodized Al at different ARB passes.

Cumulative strain accumulated in the roll-bonded samples can be given by Eq. (1),[31]

$$\varepsilon_{cum} = \varepsilon_i + 2\sqrt{3}\ln\left\{\frac{1}{2^n}\right\} \quad , \qquad (1)$$

where initial strain $\varepsilon_i = \ln\left(\frac{t_i}{t_o}\right)$, t_i = initial thickness of the sample, t_o = final thickness of the sample, and n = number of passes.

https://doi.org/10.1557/jmr.2017.176 Published online by Cambridge University Press

Cumulative strain was found to be 3.2, 4.7, and 6.3 for 1, 3, and 5 pass ARB multilayered composites, respectively. After the first pass, microhardness increased rapidly which is due to the work hardening as a result of increased dislocations density. Improvement of microhardness at higher passes of ARB is due to the combined effect of dislocation density increment and grain refinement. Microhardness of the 5-pass multilayered composite layers reached 95.2 HV (~1.25 time), 144.2 HV (~1.59 times), and 148.8 HV (~1.57 times) in comparison to its counterpart rolled Mg–6% Zn alloy, aluminum, and anodized Al, respectively. The microhardness of the multilayered composites is also affected by the presence of intermetallic ($Al_{17}Mg_{12}$ and $AlMg_4Zn_{11}$) formed during the ARB process as shown in Fig. 6. In the case of Mg–6% Zn/anodized Al multilayered composites, harder alumina particles are distributed uniformly in the microstructure during the ARB process and act as a barrier to the dislocation movement.

G. Tensile test

Variation of ultimate tensile strength (UTS), yield strength (YS), and elongation of the Mg–6% Zn/Al and

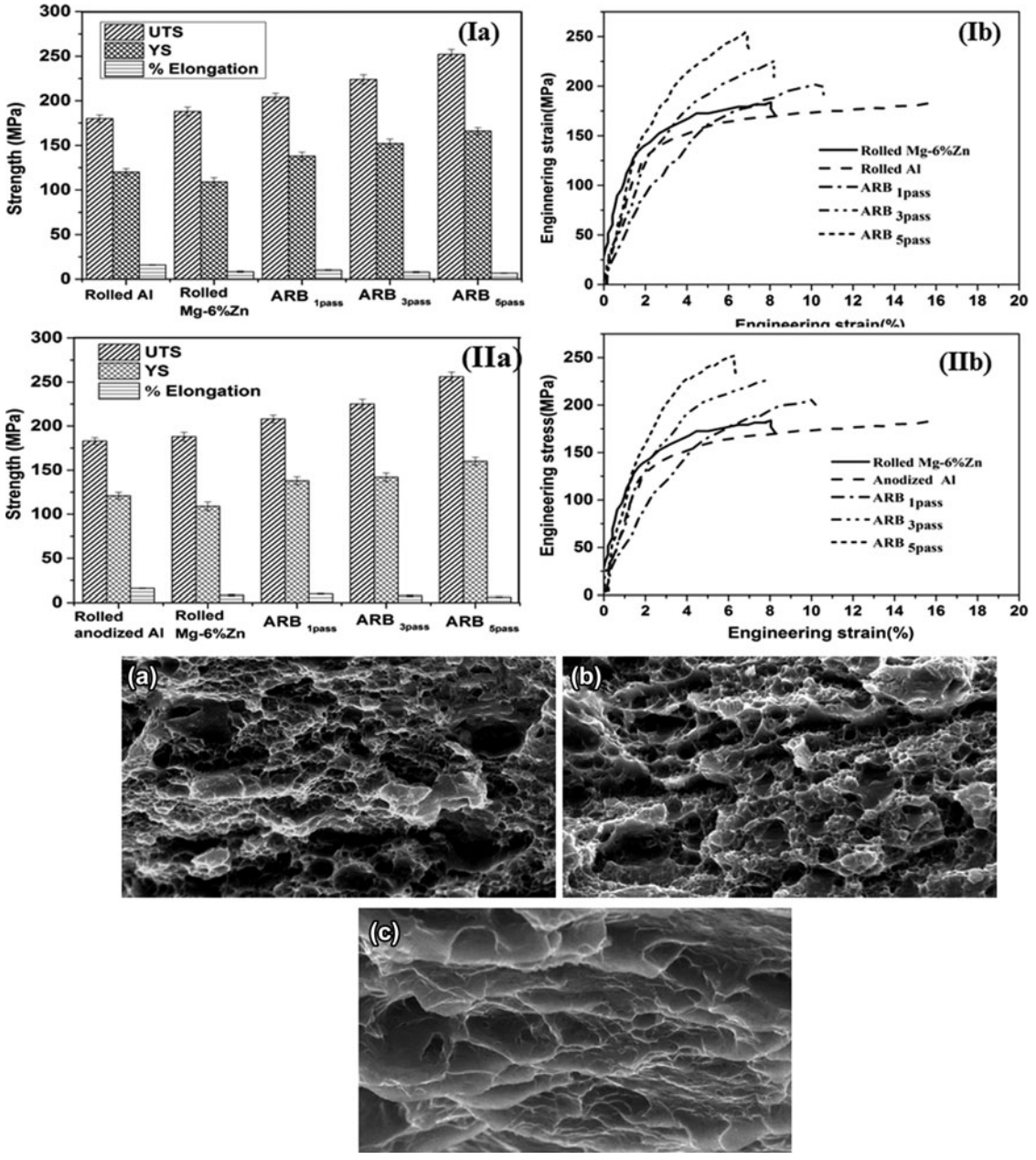


FIG. 8. Variation of UTS, YS, and percentage elongation for different passes of ARB processed multilayered composite: (Ia) Mg–6% Zn/Al, (IIa) Mg–6% Zn/anodized Al. (Ib and IIb) Engineering stress–strain curves and fracture surface of the (a) Al, (b) Anodized Al, and (c) Mg–6% Zn layers.

https://doi.org/10.1557/jmr.2017.176 Published online by Cambridge University Press

Mg–6% Zn/anodized Al multilayered composites at different ARB passes is shown in Figs. 8(I) and 8(II). As can be seen, the strength of multilayered composite increases with an increase in the number of ARB passes. The YS and UTS of the Mg–6% Zn/Al composite [Fig. 8(I)] improved to 1.52 and 1.34 times and for Mg–6% Zn/anodized Al composite [Fig. 8(II)] improved to 1.46 and 1.36 times than that of rolled Mg–6% Zn alloy, respectively. The improvement of strength in initial passes of ARB is due to strain hardening or dislocation strengthening mechanism.[32] Strength improvement at the higher ARB passes is due to the formation of fine grain structure (Hall–Petch effect), largely misoriented grain boundaries,[33] and formation of intermetallic phases.[34] At higher ARB passes, work hardening effect gradually decreases, as the number of fine grains with high angle boundaries increases. Total elongation decreases with an increasing number of ARB passes. During the initial passes, the composites exhibited higher elongation because of the presence of highly ductile element Al in the equal quantity with Mg–6% Zn. At the higher passes, the total elongation decreases due to strain hardening and refined grains. The tensile strength of the Mg–6% Zn/anodized Al composite is 1.58% higher as compared to Mg–6% Zn/Al composite due to alumina particle (due to anodization treatment). Alumina particle helps to increase the strength by pinning the dislocations and impeding their motion resulting in enhanced dislocation density and dislocation interactions which increases work hardening and strength.[35] Improved strength of the multilayered composite has been reported that it is not only the stain hardening and grain refinement but also the reinforcement effect in the matrix caused by intermetallics formed during the ARB process.[36–39] According to the Orowan mechanism, a reinforcement particle acts as a barrier to a dislocation movement. With an increase in the number of ARB passes, the density of dislocations increases along with the formation of HABs.

Fracture surface of tensile tested 5-pass ARB processed Al, anodized Al, and Mg–6% Zn layers is shown in Figs. 8(a)–8(c). Al layer and anodized Al layer in the Mg–6% Zn/Al and Mg–6% Zn/anodized Al multilayerd composite depict typical ductile failure illustrated by dimples, as shown in Figs. 8(a) and 8(b), respectively. Ductile fracture begins with the nucleation, growth, and coalescence of microvoids. The presence of shallow and small elongated microvoids affected by shear stress during ARB process confirms the shear ductile fracture. But the Mg–6% Zn layer in the multilayered composite depicts [Fig. 8(c)] bright lines on the fracture surface which are indication for cleavage fracture. Mg–6% Zn layers were fractured in the shear mode and without forming dimples which appear to be transgranular brittle fracture.

IV. CONCLUSIONS

In the present research, ARB was used to develop Mg–6% Zn/Al and Mg–6% Zn/anodized Al multilayered composites at 300 °C up to five passes successfully. Microstructural and mechanical properties of the developed composites were studied. The following conclusions can be summarized based on the obtained results.

(1) Developed Mg–6% Zn/Al and Mg–6% Zn/anodized Al multilayered composites exhibited 1.275 times and 1.274 times light weight as compared to pure Al. The formation of $Al_{17}Mg_{12}$, $AlMg_4Zn_{11}$, and Al_2O_3 intermetallics was confirmed by the XRD analysis. EBSD and TEM analyses revealed that the 5-pass ARB processed multilayered composite exhibited an average grain size of 1.8, 1.6, and 0.6 μm with high angle misorientation for Al, anodized Al, and Mg–6% Zn layers.

(2) Microhardness of the multilayered composite layers was increased with the increase in the number of ARB passes. The 5-passed composite layers exhibited 95.2 HV (~1.25 time), 144.2 HV (~1.59 times), and 148.8 HV (~1.57 times) in comparison to its counterpart rolled Mg–6% Zn alloy, aluminum, and anodized Al respectively.

(3) Tensile data indicate a significant increasing in the tensile strength of Mg–6% Zn/Al and Mg–6% Zn/anodized Al multilayered composites in comparison with the rolled Mg–6% Zn alloy due to strain hardening, grain refinement, and intermetallics formed during the ARB process. Mg–6% Zn/anodized Al composite exhibited better mechanical properties as compared to Mg–6% Zn/Al composite due to alumina particle which acts as a barrier to dislocation movement, causing enhancement of strength.

(4) Fractured surface of Al layer and anodized Al layer in the multilayered composites exhibited shear ductile failure and Mg–6% Zn layer shows cleavage, which appear to be transgranular brittle fracture.

ACKNOWLEDGMENTS

The authors gratefully appreciate the support of Department of Materials Engineering, Indian Institute of Science Bangalore, India; Advanced Center for Material Science, Indian Institute of Technology Kanpur, India; and Exclusive Magnesium Private limited, Hyderabad, India for providing various testing facilities used in this research work.

REFERENCES

1. J. Wadsworth and D.R. Lesuer: Ancient and modern laminated composites from the Great Pyramid of Gizeh to Y2K. *Mater. Charact.* **45**, 289 (2000).
2. P.H. Shingu, K.N. Ishihara, A. Otsuki, and I. Daigo: Nano-scaled multi-layered bulk materials manufactured by repeated pressing

https://doi.org/10.1557/jmr.2017.176 Published online by Cambridge University Press

and rolling in the Cu–Fe system. *Mater. Sci. Eng., A* **304**, 399 (2001).
3. A. Azushima, R. Kopp, A. Korhonen, D.Y. Yang, F. Micari, and G.D. Lahoti: Severe plastic deformation (SPD) processes for metals. *CIRP Ann. Manuf. Technol.* **57**, 716 (2008).
4. L.S. Toth and C. Gu: Ultrafine-grain metals by severe plastic deformation. *Mater. Charact.* **92**, 1 (2014).
5. A.S.J. Al-Zubaydi, A.P. Zhilyaev, S.C. Wang, and P.A.S. Reed: Super plastic behavior of AZ91 magnesium alloy processed by high-pressure torsion. *Mater. Sci. Eng., A* **637**, 1 (2015).
6. A. Muralidhar, S. Narendranath, and H. Shivananda Nayaka: Effect of equal channel angular pressing on AZ31 wrought magnesium alloys. *J. Magnesium Alloys* **1**, 336 (2013).
7. R.Z. Valiev and T.G. Langdon: Principles of equal-channel angular pressing as a processing tool for grain refinement. *Prog. Mater. Sci.* **51**, 881 (2006).
8. L.N. Tsuji and N. Kamikawa: Microstructure homogeneity in various metallic materials heavily deformed by accumulative roll-bonding. *Mater. Sci. Eng., A* **423**, 331 (2006).
9. M.M. Mahdavian, L. Ghalandari, and M. Reihanian: Accumulative roll bonding of multilayered Cu/Zn/Al: An evaluation of microstructure and mechanical properties. *Mater. Sci. Eng., A* **579**, 99 (2013).
10. S. Roy, B.R. Nataraj, S. Suwas, S. Kumar, and K. Chattopadhyay: Microstructure and texture evolution during accumulative roll bonding of aluminium alloys AA2219/AA5086 composite laminates. *J. Mater. Sci.* **47**, 6402 (2012).
11. Y. Xin, R. Hong, B. Feng, H. Yu, Y. Wu, and Q. Liu: Fabrication of Mg/Al multilayer plates using an accumulative extrusion bonding process. *Mater. Sci. Eng., A* **640**, 210 (2015).
12. M. Tayyebi and B. Eghbali: Study on the microstructure and mechanical properties of multilayer Cu/Ni composite processed by accumulative roll bonding. *Mater. Sci. Eng., A* **559**, 759 (2013).
13. D.W. Lee and B.K. Kim: Nanostructured Cu–Al_2O_3 composite produced by thermochemical process for electrode application. *Mater. Lett.* **58**, 378 (2004).
14. H.S. Liu, B. Zhang, and G.P. Zhang: Microstructures and mechanical properties of Al/Mg alloy multilayered composites produced by accumulative roll bonding. *J. Mater. Sci. Technol.* **27**, 15 (2011).
15. H. Matsumoto, S. Watanabe, and S. Hanada: Sheet cladding of Al–Mg/Mg–Li/Al–Mg at room temperature. *Mater. Sci. Forum* **29**, 446 (2005).
16. M. Eizadjou, A.K. Talachi, H.D. Manesh, H.S. Shahabi, and K. Janghorban: Investigation of structure and mechanical properties of multi-layered Al/Cu composite produced by accumulative roll bonding (ARB) process. *Compos. Sci. Technol.* **68**, 2003 (2008).
17. H. Chang, M. Zheng, W. Gan, C. Xu, and H.G. Brokmeier: Texture evolution of the Mg/Al laminated composite by accumulative roll bonding at ambient temperature. *Rare Met. Mater. Eng.* **42**, 0441 (2013).
18. M.C. Chen, H.C. Hsieh, and W.T. Wu: The evolution of microstructures and mechanical properties during accumulative roll bonding of Al/Mg composite. *J. Alloys Compd.* **416**, 169 (2006).
19. H. Inoue, M. Ishio, T. Takasugi, H. Inoue, M. Ishio, and T. Takasugi: Texture of TiNi shape memory alloy sheets produced by roll-bonding and solid phase reaction from elementary metals. *Acta Mater.* **51**, 6373 (2003).
20. H.S. Ding, J.M. Lee, B.R. Lee, S.B. Kang, and T.H. Nam: Processing and microstructure of TiNi SMA strips prepared by cold roll-bonding and annealing of multilayer. *Mater. Sci. Eng., A* **408**, 182 (2005).
21. D. Yang, P. Cizek, P. Hodgson, and C.E. Wen: Ultrafine equiaxed-grain Ti/Al composite produced by accumulative roll bonding. *Scr. Mater.* **62**, 321 (2010).
22. X.X. Yu and W.B. Lee: The design and fabrication of an alumina reinforced aluminum composite material. *Composites, Part A* **31**, 245 (2000).
23. R. Jamaati, M.R. Toroghinejad, and A. Najafizadeh: High-strength and highly-uniform composite produced by anodizing and accumulative roll bonding processes. *Mater. Des.* **31**, 4816 (2010).
24. M.R. Toroghinejad, R. Jamaati, A. Nooryan, and H. Edris: The effect of alumina content on the mechanical properties of hybrid composites fabricated by ARB process. *Ceram. Int.* **40**, 10489 (2014).
25. Z.P. Xing, S.B. Kang, and H.W. Kim: Microstructural evolution and mechanical properties of the AA8011 alloy during the accumulative roll-bonding process. *Metall. Mater. Trans. A* **33**, 1521 (2002).
26. R. Jamaati and M.R. Toroghinejad: Effect of SFE on mechanical properties of nanostructured FCC materials processed by the ARB process. *Mater. Sci. Eng., A* **606**, 443 (2014).
27. F.J. Humphreys and M. Hatherly: *Recrystallization and Related Annealing Phenomena*, 2nd ed. (Elsevier, Australia, 2004); p. 457.
28. N. Hansen and D.J. Jensen: Deformed metals structure, recrystallisation and strength. *Mater. Sci. Technol.* **27**, 1229 (2002).
29. S.H. Lee, Y. Saito, N. Tsuji, H. Utsunomiya, and T. Sakai: Role of shear strain in ultragrain refinement by accumulative roll-bonding (ARB) process. *Scr. Mater.* **46**, 281 (2002).
30. Y. Chino, K. Kimura, and M. Mabuchi: Twinning behavior and deformation mechanisms of extruded AZ31 Mg alloy. *Mater. Sci. Eng., A* **486**, 481 (2008).
31. Y. Saito, H. Utsunomiya, N. Tsuji, and T. Sakai: Novel ultra-high straining process for bulk materials development of the accumulative roll-bonding (ARB) process. *Acta Mater.* **47**, 579 (1999).
32. N. Hansen, X. Huang, R. Ueji, and N. Tsuji: Structure and strength after large strain deformation. *Mater. Sci. Eng., A* **387**, 191 (2004).
33. D. Terada, S. Inoue, and N. Tsuji: Microstructure and mechanical properties of commercial purity titanium severely deformed by ARB process. *J. Mater. Sci.* **42**, 1673 (2007).
34. C.W. Schmidt, C. Knieke, V. Maier, H.W. Hopple, W. Peukert, and M. Goken: Accelerated grain refinement during accumulative roll bonding by nanoparticle reinforcement. *Scr. Mater.* **64**, 245 (2011).
35. R. Jamaati, M.R. Toroghinejad, J. Dutkiewicz, and J.A. Szpunar: Investigation of nanostructured Al/Al_2O_3 composite produced by accumulative roll bonding process. *Mater. Des.* **35**, 37 (2012).
36. H. Chang, M.Y. Zheng, C. Xu, G.D. Fan, H.G. Brokmeier, and K. Wu: Microstructure and mechanical properties of the Mg/Al multilayer fabricated by accumulative roll bonding (ARB) at ambient temperature. *Mater. Sci. Eng., A* **543**, 249 (2012).
37. D.M. Parisa and E. Beitallah: Microstructure and mechanical properties of tri-metal Al/Ti/Mg laminated composite processed by accumulative roll bonding. *Mater. Sci. Eng., A* **628**, 135 (2015).
38. R. Jamaati and M.R. Toroghinejad: Manufacturing of high strength aluminum–alumina composite by accumulative roll bonding. *Mater. Sci. Eng., A* **527**, 4146 (2010).
39. A. Ahmadi, M.R. Toroghinejad, and A. Najafizadeh: Evaluation of microstructure and mechanical properties of Al/Al_2O_3/SiC hybrid composite fabricated by accumulative roll bonding process. *Mater. Des.* **53**, 13 (2014).

https://doi.org/10.1557/jmr.2017.176 Published online by Cambridge University Press